Experimental Investigation of Wing/Fuselage Integration Geometries

M. Maughmer,* D. Hallman,† R. Ruszkowski,‡ G. Chappel,§ and I. Waitz¶
Pennsylvania State University, University Park, Pennsylvania

Although long recognized as a significant contributor to overall drag, a great deal of work yet remains to be done on understanding and controlling the interference flowfield generated by the wing/fuselage intersection. One possible means of reducing the drag due to this interference is through the careful blending of the wing/fuselage region near the front of the juncture. To investigate such wing/fuselage integration, an experimental program has been performed in which flow visualization, pressure distributions, and force-balance data were obtained and used to explore promising junction geometries. These experiments indicate that the juncture flow is very sensitive to the wing/fuselage intersection geometry, and that the proper shaping of this region can lead to a reduction in interference drag.

Nomenclature

C_D = drag coefficient
C_L = lift coefficient
R = Reynolds number based on freestream conditions and the mean aerodynamic chord
x/c = fraction of wing chord
x/L = fraction of fuselage length
α = angle of attack relative to the chord line of the wing

Introduction

As the use of composite materials in aircraft structures becomes commonplace, it makes sense to exploit the aerodynamic benefits offered by sometimes complicated geometries. Likewise, as the potential for such aerodynamic tailoring becomes realizable, the need for understanding exactly how to take advantage of these capabilities becomes more and more critical. In this regard, although attempts to model the aerodynamics in the region of the wing/fuselage intersection have been ongoing for many years, efforts to actually tailor this juncture in order to minimize the interference drag are more recent. For example, a number of efforts to improve the wing/fuselage aerodynamics have been directed toward sailplanes because of the high premium placed on performance gains, and the widespread use of composites has allowed these gains to be realized. As shown in Refs. 1–4, these efforts primarily explore the effects of fuselage shape and wing location. Other recent activities have been of a more general nature and are applicable to the design of all subsonic aircraft. For example, the influence of the airfoil section on the juncture flow is reported in Ref. 5, and the suggestion was made that the section used in the wing-root region be chosen specifically to operate in the flow conditions found there. The importance of the leading-edge shape on the size and strength of the vortex that forms in the wing/fuselage intersection is discussed in Refs. 6 and 7. Improving the juncture flow by extending the wing leading edge in the root region is explored experimentally in Refs. 8–10 and numerically in Ref. 11. Unlike conventional filleting, which attempts to reduce the interference drag by merging the wing and fuselage flows as smoothly as possible, the intent of leading-edge fairings is to suppress the formation of the vortex that forms in the wing/fuselage juncture. The goal is, of course, to obtain an interference drag reduction that more than offsets the increased skin-friction drag due to the fairing.

Although not making use of a blending fairing, the effort of Boermans and Waibel[12] is a notable attempt to design a wing/fuselage intersection such that the interference drag is minimized. In particular, a potential flow code (panel method) is used to determine a configuration for which the large positive pressures due to the fuselage contraction are combined with the large negative pressures induced by the wing such that strong adverse pressure gradients are avoided. Further, whereas the rest of the wing incorporates a laminar-flow section, the airfoil used in the region of the wing/fuselage junction is designed specifically for the turbulent flow anticipated there.

In order to gain insight into the wing/fuselage intersection flow phenomena and to examine the potential of geometrically blending the wing and fuselage to improve the juncture aerodynamics, a series of wind-tunnel experiments have been conducted.[13,14] These efforts have included flow visualization, pressure distribution determination, and direct lift and drag force measurements. Rather than examine wing/body aerodynamics using an idealized geometry, as was the case in several previous studies, the phenomena is explored using a realistic wing/fuselage configuration. The baseline configuration is provided by the 15-m-span sailplane depicted in Fig. 1. Although the results of this study are applicable to any number of aircraft types, the decision to use a sailplane wing/body combination was made in part because the wind tunnel employed in these experiments is limited in its ability of achieving high Reynolds numbers. Thus, the measurements are more typical of a full-scale sailplane than would be expected for most other types of aircraft. Furthermore, the use of a sailplane is attractive in that the design of the wing/body region for such aircraft has already received a considerable amount of attention and, consequently, has been refined to a fairly high level. Thus, any performance gains achieved

Received Aug. 10, 1987; presented as Paper 87-2937 at the AIAA/AHS/ASEE Aircraft Design and Operations Meeting, St. Louis, MO, Sept. 14–16, 1987; revision received Feb. 25, 1989.

*Assistant Professor, Department of Aerospace Engineering. Member AIAA.
†Undergraduate Student, Department of Aerospace Engineering, Student Member AIAA; currently, Engineer, General Dynamics Corp., Fort Worth, TX.
‡Undergraduate Student, Department of Aerospace Engineering; Student Member AIAA; currently, Senior Engineer, General Dynamics Corp., Fort Worth, TX.
§Undergraduate Student, Department of Aerospace Engineering, Student Member AIAA; currently, Lieutenant, Electronics Warfare Officer, U.S. Air Force, Minot, ND.
¶Undergraduate Student, Department of Aerospace Engineering; Student Member AIAA; currently, Graduate Student, Department of Aeronautics, California Institute of Technology, Pasadena, CA.

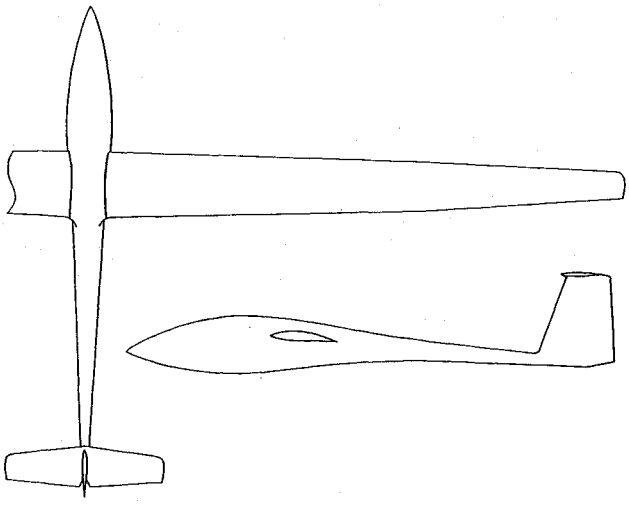

Fig. 1 Fifteen-m-span sailplane used in wing/fuselage juncture-flow experiments.

through wing/fuselage integration would be of considerable significance.

Wing/Fuselage Juncture Flows

Although more detailed discussions can be found in Refs. 15 and 16, it is helpful to review certain aspects of juncture flows in order to understand how the situation can be improved through wing/fuselage integration. The most significant aerodynamic features can be considered as those due to the effects of lift, displacement, viscosity, and asymmetry.

Lift effects arise from circulatory flows around the wing and fuselage. Although insufficient to predict the interaction, these effects can be explained by considering the wing as a line vortex that intersects the fuselage normally. From this simple model, it is clear that upwash is induced on the fuselage ahead of the vortex line, whereas downwash is induced behind it. As a consequence of the interaction between the flow over the wing with that over the fuselage, the chordwise and spanwise load distributions of the isolated wing are altered considerably when in the proximity of the body. Likewise, the pressure distribution around the body is altered by the presence of the wing.

Displacement effects are due to the fact that, because the wing has thickness, the intersection lines between the wing and fuselage are curved. Consequently, provided the flow follows the curved intersection lines, an interference velocity is introduced. To minimize these effects, although strictly applicable to only a single flight condition, it has sometimes been advocated that the fuselage be shaped to conform to the streamlines of the wing. Alternatively, it has been suggested that thin, sharp wing leading edges will help to reduce the displacement effect; however, this also limits the angle-of-attack range somewhat.[6]

For a thin wing joined to an axisymmetric fuselage at zero angle of attack in inviscid flow, lift and displacement effects are insignificant. In the real flow, however, the aerodynamic interference would still be strong due to the presence of viscous effects. These effects are caused primarily by the interaction between the boundary layers on the two intersecting surfaces. The boundary layer along the fuselage separates as it runs up against the strong adverse pressure gradient encountered as the wing leading edge is approached. As idealized in Fig. 2, a line of separated flow wraps around the junction beginning from the stagnation point on the body just upstream of the wing. The free edge of the separated region then rolls up on either side of the wing forming a vortex that trails back along the upper and lower surfaces of the intersection.

Finally, while the three effects discussed thus far are present to some extent in all wing/body flows of practical interest, the aerodynamics are further influenced if the juncture is not symmetrical. For example, if the wing is cambered or set at incidence relative to the body, the intersection lines along the upper and lower surfaces are not the same. In this case, the induced interference velocities on the upper and lower surfaces are different. This effect can be further aggravated if the wing is not mounted on the fuselage centerline, or by dihedral sweep, and so forth.

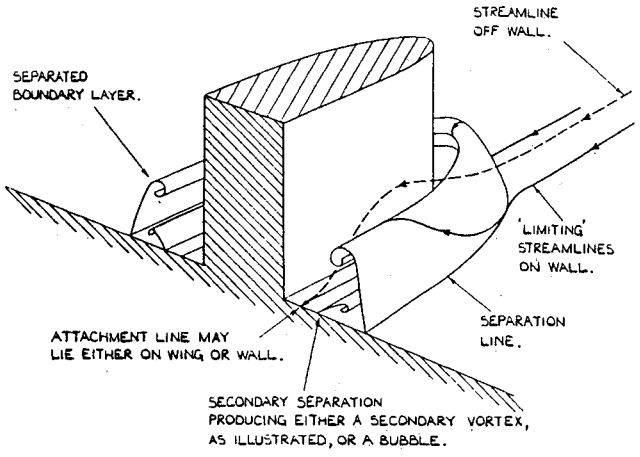

Fig. 2 The flowfield in an idealized wing/fuselage juncture.[17]

In considering minimizing interference in the wing/fuselage intersection, the importance of fuselage shape and wing placement in eliminating strong adverse pressure gradients and the resulting separated flow is clear. Furthermore, although conventional filleting has been successful in reducing the viscous effects, more recent work employing geometrical wing/fuselage integration has shown promise for actually controlling the formation of the intersection vortex system. This is accomplished primarily through the blending of the wing/fuselage juncture by extending the wing leading edge in the root region. The smoother transition between the fuselage and the wing reduces the impact of the displacement effect by spreading it out over a greater length. This, in turn, lessens the adverse pressure gradients that cause the flow to separate and form the intersection vortex system. In this manner, the size and strength of the vortex system can be reduced. Lastly, the additional area near the wing roots helps to recover a portion of the lift that is typically lost in the region of the intersection.

Description of Experimental Program

Models and Test Conditions

Two wind-tunnel models were used in the course of the wing/fuselage juncture flow studies. The model used for flow visualization studies and force-balance data is one-fourth scale. It is symmetrical about the fuselage centerline and has wings, truncated at 0.4 of full span, which effectively span the wind-tunnel test section. With this model, it is possible to achieve Reynolds numbers based on the mean aerodynamic chord of 400,000. In addition to the baseline geometry, the model can be modified through the use of six different wing/fuselage integration geometries. These geometries consist of the three profile and front views shown in Fig. 3. Each of these, in turn, was developed with both the parabolic and linear planforms shown in Fig. 4. The most promising integration geometries for reducing the juncture drag—integration geometry with both the parabolic (−A) and linear (−B) planforms—are based on the findings of Refs. 6 and 7. These geometries are created by extending the airfoil leading-edge shape forward. The other geometries were selected to explore the impact of increasingly blunter leading-edge shapes on the intersection aerodynamics. Effectively, these geometries are formed by extending the leading edge forward and fairing the resulting shape more and more toward the fuselage. As no attempt is made to retain the original airfoil leading-edge shape, the resulting leading edge is rounded considerably as the ge-

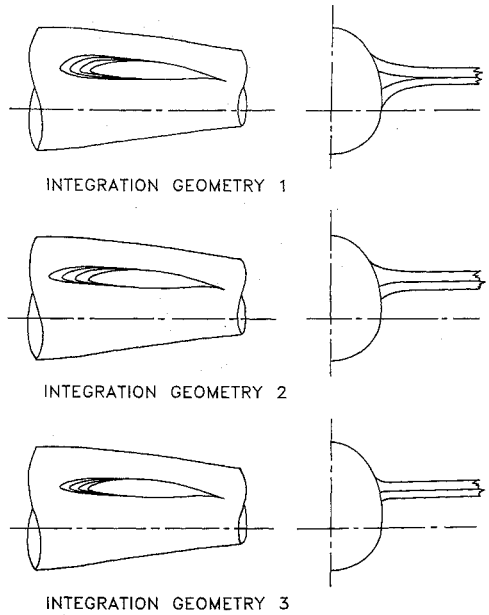

Fig. 3 Profile and front views of wing/fuselage integration geometries.

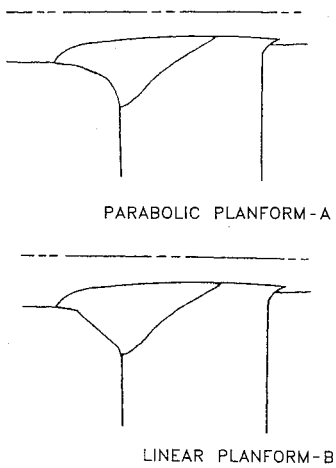

Fig. 4 Planform views of wing/fuselage integration geometries.

ometry is blended to the fuselage. The two planform shapes were chosen to more fully explore the range of possible integration configurations.

The model used to obtain pressure distribution data is of one-seventh scale. Although this model is asymmetrical, having one wing truncated at 15% of the semispan, flow visualization studies demonstrate that the effects of the asymmetry have little influence on the flow in the region of the fuselage. This model was tested at a Reynolds number based on the mean aerodynamic chord of 250,000. In addition to the baseline configuration, this model was tested with an integration geometry having a blunt-nosed leading-edge extension and a parabolic planform, geometry 1-A, in place.

The flow visualization and pressure distribution studies were conducted at angles of attack relative to the wing chordline of -1.0 deg, corresponding to the interthermal cruising flight of the sailplane, and at $+4.5$ deg, corresponding to low-speed thermaling flight. Except as noted, the full-scale boundary-layer transition locations, obtained from Ref. 18 were achieved on the wing and fuselage of the model using trip tape. Although the actual transition locations vary with angle of attack, to simplify the experimental procedure most of the tests were performed with the trip tape positioned at locations corresponding to cruising flight. Conducting the experiments in this manner should have little influence on the results over a fairly wide range of angles of attack, because the full-scale transition locations do not move a great deal as long as the aircraft components are operating within the laminar drag bucket. Likewise, although full-scale transition occurs through the formation of laminar separation bubbles, altering the transition mechanism should have little influence on the wing/body flow phenomena.

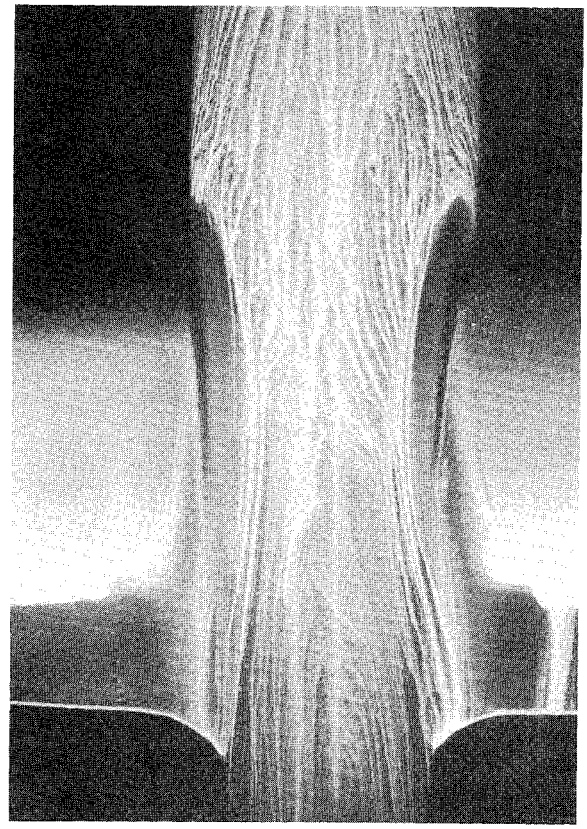

Fig. 5 Planview oilflow visualization of the wing/fuselage juncture flow with natural transition, $\alpha = 4.5$ deg.

Wind Tunnel

All of the experiments in this program were conducted in the low-speed wind tunnel of the Department of Aerospace Engineering at the Pennsylvania State University. This is a closed-return tunnel having a 4×5 ft rectangular test section. The test-section turbulence level of this facility at the velocities of the wing/fuselage experiments is about 0.4%. For these measurements, because the boundary-layer transition is fixed by trips, the level of turbulence is not likely to have a strong influence on the results. To obtain force measurements, the tunnel is equipped with a six-component, pyramidal balance. The standard wind-tunnel boundary corrections, as given in Ref. 19, have been applied to all force-balance data.

Results and Discussion

Flow Visualization

Before the transition strips were put in place, fluorescent oil flow studies were performed on the baseline model with interesting results. A comparison of these results with those for fixed transition is represented by the planform view of the two juncture flows given in Figs. 5 and 6. The natural transition case is characterized by the presence of large laminar separation bubbles on the wings. These bubbles extend from the laminar separation line at $x/c = 0.5$, which is difficult to observe in the black and white photographs, to turbulent reattachment clearly visible at about $x/c = 0.75$. As expected, a large amount of spanwise flow occurs along the trailing edge in the region of turbulent separated flow that can be seen there. The flowfield in the case of natural transition is the result of the laminar

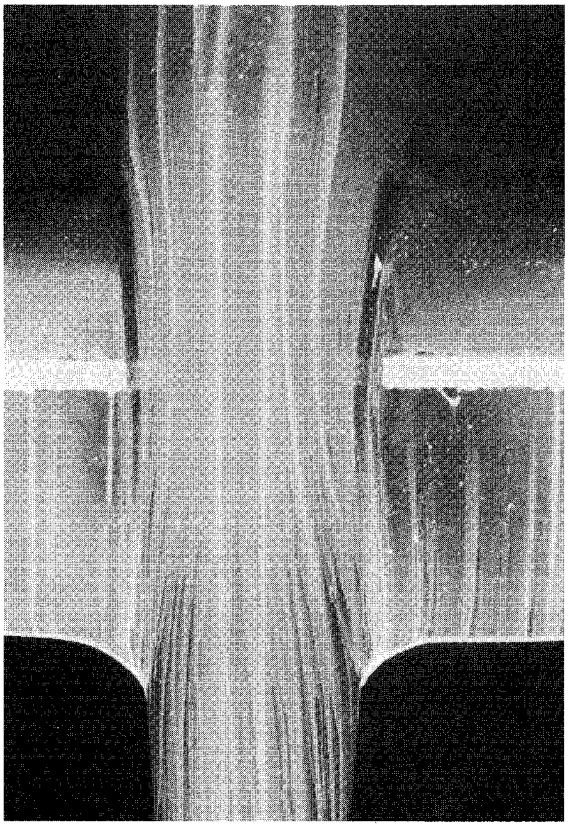

Fig. 6 Planview oilflow visualization of the wing/fuselage juncture flow with fixed transition, $\alpha = 4.5$ deg.

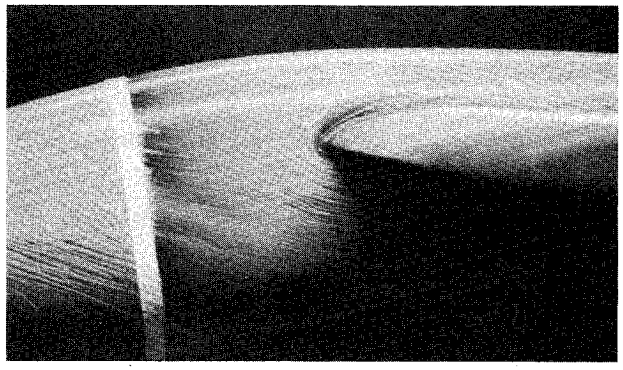

Fig. 7 Oilflow visualization of the stagnation point and juncture vortex formation, $\alpha - 1$ deg.

boundary layer on the fuselage flowing into the region of the wing/fuselage juncture. The presence of the vortex system that forms near the leading edge and flows back into the intersection is indicated by the dark bands created when the strong surface shearing forces scrub the oil from the surface in those regions.

As they do with transition free, the curved intersection streamlines observed in the planview of the fixed-transition intersection clearly demonstrate the displacement effect on the juncture flow phenomena discussed earlier. Otherwise, the fixed transition flow is quite different from that having natural transition. The transition strips on the upper surface of the wings are seen near $x/c = 0.75$. In this case, the formation of juncture flow involves a turbulent boundary layer on the fuselage. Compared to the case having natural transition, the vortex forming in the juncture when transition is fixed is considerably smaller and its influence on the surrounding flowfield significantly less. Unlike in the free transition case, the vortex detaches from the upper side of the intersection long before the trailing edge is reached. Clearly, in conducting

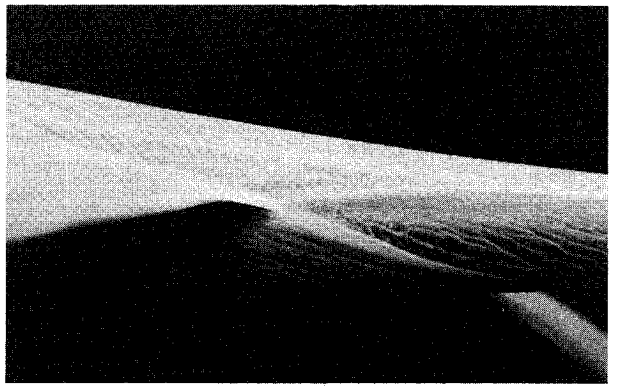

Fig. 8 Oilflow visualization of the flow in the trailing-edge region of the wing/fuselage intersection, $\alpha = 4.5$ deg.

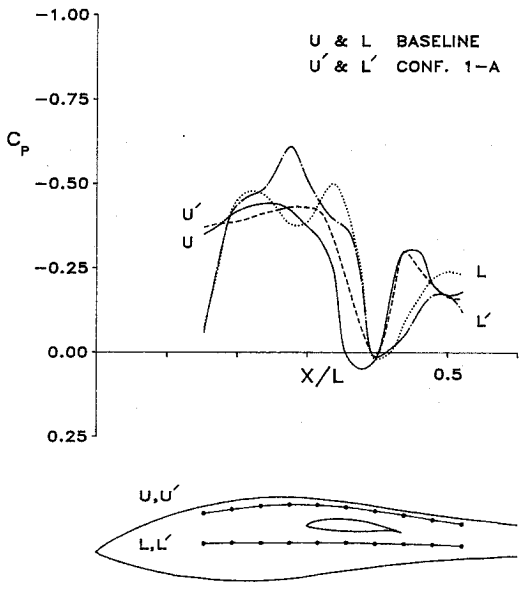

Fig. 9 Comparison of pressure distributions along fuselage lines for baseline and modified configurations, $\alpha - 1$ deg.

experiments aimed at improving wing/fuselage juncture flows, it is important that the fuselage boundary layer that flows into the wing juncture be properly simulated. The specific geometry that improves a laminar intersection is likely to be very different from that designed for a turbulent juncture.

For the baseline configuration with tripped boundary layers, the stagnation point that forms on the fuselage upstream of the wing/fuselage intersection at the angle of attack corresponding to cruising flight is seen in Fig. 7. Although the low angle of attack in this case causes the stagnation point to be above the leading edge, it is otherwise typical of those seen at all angles of attack. The formation and turning back of the vortex system into the wing-root region is also evident in this photograph.

The trailing-edge region of the wing/fuselage junction is shown in Fig. 8. The intersection of vortical flow with the fuselage as well as adjacent lines of separation is marked by the characteristic v-pattern that appears to emanate from the trailing edge. This pattern, as observed by past researchers and discussed in detail in Ref. 20, is thought to be caused by the secondary vortex flows originating at the leading edge, as illustrated in Fig. 2, which are transported along the wing/body junction to the trailing edge. Fluorescent oil flow studies were also conducted with the various integration geometries in place. Although in some cases the influence of the intersection vortex on the surrounding flowfield appears to be somewhat diminished, the overall behavior of the juncture flow is similar to that shown for the baseline configuration.

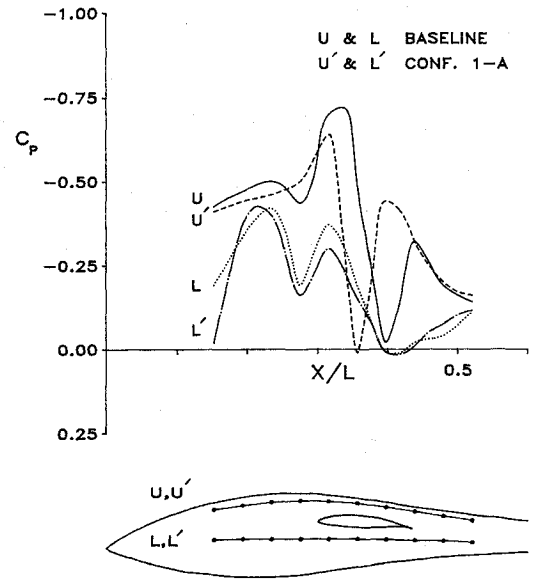

Fig. 10 Comparison of pressure distributions along fuselage lines for baseline and modified configurations, $\alpha = +4.5$ deg.

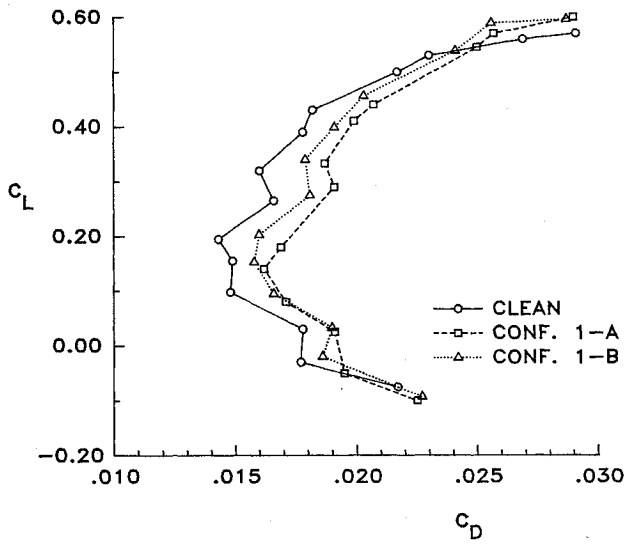

Fig. 11 Drag polar comparison of baseline sailplane to those modified using integration geometry 1, $R = 400{,}000$.

Pressure Distributions

The fuselage pressure distributions for the baseline one-seventh-scale model at angles of attack corresponding to cruising and thermaling flight are shown in Figs. 9 and 10, respectively. For comparison, the pressure distributions for the model modified with integration geometry (1-A) are also presented in each figure. The pressure distribution lines plotted correspond to the two rows of orifices along the fuselage sides indicated in the figure. The positions of the orifices along the fuselage are also shown. Although the orifice rows clearly do not correspond exactly with streamlines, panel method studies indicate that the pressure gradients along the orifice lines are not greatly different from those along the streamlines over that region of the fuselage.

The pressure distribution lines for the baseline configuration at the cruising angle of attack shown in Fig. 9 are characterized by adverse pressure gradients near $x/L = 0.2$, corresponding to the start of the contraction of the body shape. At this low angle of attack, the influence of the wing flowfield does not appear strongly felt along the upper body line. On the underside of the wing, the interaction of the wing flowfield with that of the fuselage crossflow, which is resulting from a

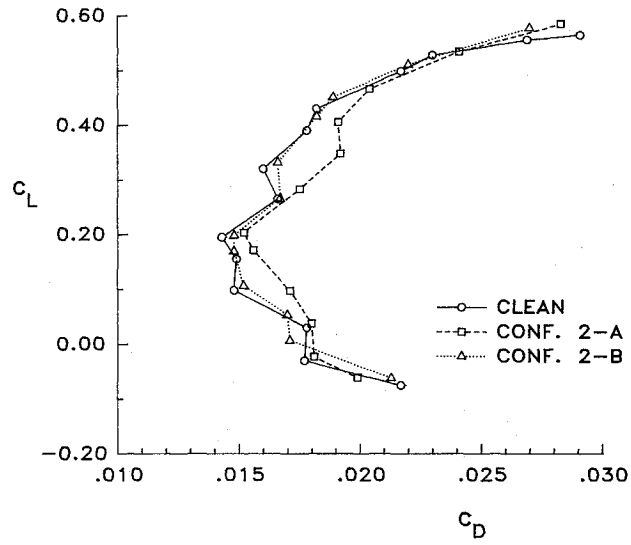

Fig. 12 Drag polar comparison of baseline sailplane to those modified using integration geometry 2, $R = 400{,}000$.

negative angle of attack in this case, is observed. As the trailing edge of the wing is approached, the pressure recovery on the wing combined with that on the fuselage, due to its waisting in that region, is responsible for the steep adverse pressure gradients present along both body lines. Downstream of the trailing edge, the body lines are seen to have favorable pressure gradients, possibly due to the acceleration of the flow caused by the reconverging of the streamline now past the influence of the wing displacement effect.

Although the magnitudes of the pressure peaks and the steepness of the gradients are all greater, the pressure distribution patterns corresponding to the baseline configuration at the thermaling angle of attack, shown in Fig. 10, are similar to those of Fig. 9. Most of the differences observed are because the fuselage crossflow is now the result of a positive body angle of attack. Also, the vortex shed from the underside of the wing/fuselage juncture at the trailing edge now influences the pressures along line L.

In comparing the pressure distributions for the baseline and the modified configurations at the cruising angle of attack as presented in Fig. 9, the adverse pressure gradients upstream of the leading edge due to the contraction of the fuselage in the baseline case are seen eliminated by the integration fairing. In addition, the adverse gradients that appear downstream of the wing trailing edge on the baseline configuration are somewhat less steep.

For thermaling flight presented in Fig. 10, the comparison between the baseline and modified configurations is similar to that of cruising flight. In this case, however, the integration fairing eliminates the adverse pressure gradient due to the contraction of the fuselage only on the upper body line.

Force Measurements

Although pressure measurements suggest that the pressure distributions are "smoother" with the integration geometries in place, they do not provide any information as to whether or not the overall drag is reduced. Thus, lift and drag force balance measurements were performed. In addition to the unmodified sailplane, lift and drag data were taken with the six different wing/fuselage integration geometries previously described in place. The results of these measurements have been reduced to coefficient form and presented as drag polars in Figs. 11–13. As the coefficients are based on the wing area of the truncated model, the polars are only useful for comparison purposes and are in no way representative of the flight polars for the full-scale aircraft.

Each of the polars shown in Figs. 11–13 represents the average of a number of separate runs and, because of the high

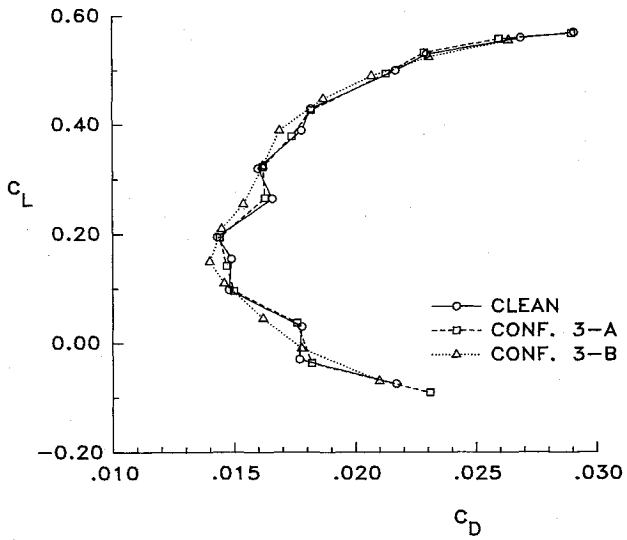

Fig. 13 Drag polar comparison of baseline sailplane to those modified using integration geometry 3, $R = 400{,}000$.

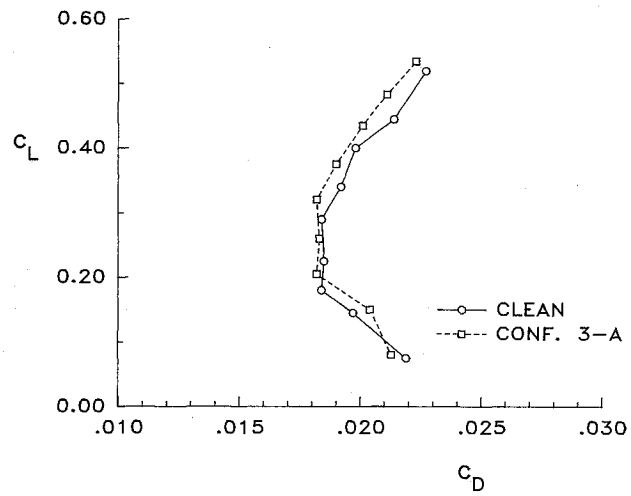

Fig. 14 Drag polar comparison of baseline sailplane to that modified using integration geometry 3-A, $R = 230{,}000$.

degree of repeatability between these runs, there is a high degree of confidence in the accuracy of the comparisons. For example, although the "bumps" present in the baseline polar might be thought due to instrumentation inaccuracies because these characteristics are present in the 17 separate runs for which the polar given is a composite, it is felt that this is not the case. More likely, the bumps are due to such things as the influences of the formation and bursting of laminar separation bubbles on the flow over various components of the test model.

Perhaps the most unexpected result of the force balance measurements is the large impact of the relatively small integration fairings on the overall drag of the model. Unfortunately, most of this dramatic impact is in the direction of increased drag. The worst of these cases is that of integration geometry 1-A, as shown in Fig. 11. For this case, there is an increase in drag of as much as 15% at nearly all points on the polar of interest.

As seen in Figs. 11 and 12, the blunt-nosed integration geometries have only slightly better performance than the unmodified sailplane at very high-lift coefficients and produces some penalty at lower-lift coefficients. Fortunately, however, as shown in Fig. 13, integration geometries 3-A and 3-B, which were expected to give the best results, demonstrate some encouraging performance in the range of lift coefficients of interest. The root leading-edge extension geometry, having a parabolic planform (3-A), achieves essentially "break-even" performance with the baseline, whereas the linear planform (3-B), obtains a 3–5% drag reduction over much of the polar. That this geometry is most successful is consistent with the theoretical findings of Ref. 6, which indicate that a low-thickness ratio in the root is most desirable. Furthermore, that this geometry provided the best wing-juncture treatment is also in agreement with the findings of Ref. 9. In that effort, similar geometries were wind-tunnel tested; however, not only were the wing and fuselage geometries idealized, but the tests were run at low Reynolds numbers, and the untripped fuselage boundary layer was laminar as it flowed into the wing/fuselage intersection. The present study confirms those results using realistic wing and fuselage shapes and with a turbulent juncture flow. In generalizing the preceding results, it is found that the linear planform yields superior performance to the parabolic one in every case. With respect to the leading-edge shape of the integration geometries, the performance increases as the leading edge becomes sharper. In fact, it is likely that the optimum drag reduction for the sailplane configuration of this study occurs with a smaller integration fairing than tested.

To explore the influence of Reynolds number on the wing/fuselage flow, in addition to the tests conducted at $R = 4.0 \times 10^5$, measurements were also obtained for the baseline configuration and integration geometry 3-A at $R = 2.3 \times 10^5$. The drag polars resulting from these two transition fixed runs are presented in Fig. 14. These measurements indicate that the benefits of the integration fairing are even greater as the Reynolds number is decreased. As suggested by the flow visualizations of Figs. 5 and 6, this result might be expected in that the influence of the intersection vortex on the juncture flowfield increases as the fuselage boundary layer becomes relatively thicker. Thus, as the Reynolds number is decreased, the juncture flow is more and more dominated by viscous effects.

Concluding Remarks

Clearly, the most significant finding of the wing/fuselage juncture flow experiments is that it is possible to reduce the intersection drag through the use of blending, integration fairings. Using the force-balance results in a drag buildup to estimate the impact such integration fairings would have on a full-scale, full-winged sailplane, it is found that they can provide a 2–3% decrease in drag for a vehicle that is already aerodynamically very clean.

Regarding the specific integration geometry shapes, a linear planform integration produces better results than a parabolic one. Furthermore, as consistent with theoretical and experimental results of previous efforts, a sharp-nosed fairing that extends the root section in the direction of the leading edge has significantly better performance than a blunted geometry.

Although the potential of wing/fuselage integration has been demonstrated, a great deal remains to be done to determine the most suitable geometries, the maximum performance gains achievable, the tradeoffs required for off-design conditions, and so forth. The experiments of this program confirm the notion that wing/fuselage juncture flows are, indeed, complicated. The complete modeling of such flows remains difficult and must include viscous effects and account for three-dimensional boundary-layer behavior. On the basis of the flow visualizations, however, it is apparent that the juncture flows representative of full-scale aircraft are dominated by displacement and fuselage crossflow effects. Thus, with experience and an innovative approach, it should be possible to use existing inviscid-flow design tools, such as three-dimensional panel methods and integral boundary-layer methods along streamlines, to significantly improve the aerodynamics and performance of wing/body combinations.

References

[1]Althaus, D., "Wind Tunnel Measurements on Bodies and Wing-Body Combinations," *Motorless Flight Research, 1972,* NASA CR-2315, Nov. 1973, pp. 159–178.

[2]Ostrowski, J., Litwinczyk, M., and Turkowski, L., "Flow Phenomena Along Fuselage and Wing-Fuselage Systems of Gliders," NASA TM-75401, Dec. 1980 (translated from *Archiwum Budowy Maszyn,* Vol. 25, No. 1, 1978, pp. 91-104).

[3]Radespiel, R., "Wind Tunnel Investigations of Glider Fuselages with Different Waistings and Wing Arrangements," NASA TM-77014, Jan. 1983 (translated from *Akademische Fliergergruppe Braunschweig,* West Germany, 1981, pp. 1-13).

[4]Boermans, L. M. M. and Terleth, D. C., "Wind Tunnel Tests of Eight Sailplane Wing-Fuselage Combinations," *Technical Soaring,* Vol. VIII, No. 3, Feb. 1984, pp. 70-85.

[5]Ross, J. C., Vogel, J. M., and Corsiglia, V. R., "Full-Scale Wind-Tunnel Study of Wing-Fuselage Interaction and Comparison with Paneling Method," AIAA Paper 81-1666, Aug. 1981.

[6]Mehta, R. D., "Effect of Wing Nose Shape on the Flow in a Wing/Body Junction," *Aeronautical Journal,* Vol. 88, No. 880, Dec. 1984, pp. 456-460.

[7]Kubendran, L. R., McMahon, H. M., and Hubbartt, J. E., "Turbulent Flow Around a Wing-Fuselage Type Juncture," AIAA Paper 85-0040, Jan. 1985.

[8]Jupp, J. A., "Interference Aspects of the A310 High Speed Wing Configuration," *Subsonic/Transonic Configuration Aerodynamics,* AGARD CP-285, Paper No. 11, Sept. 1980, pp. 11.1-11.16.

[9]Kubendran, L. R. and Harvey, W. D., "Juncture Flow Control Using Leading-Edge Fillets," AIAA Paper 85-4097, Oct. 1985.

[10]Harvey, W. D., "Low-Reynolds Number Aerodynamics Research at NASA Langley Research Center," *Aerodynamics at Low Reynolds Numbers,* Conference Proceedings, Vol. II, Royal Aeronautical Society, London, Oct. 1986, pp. 19.1-19.49.

[11]Sung, C. H. and Lin, C. W., "Numerical Investigation on the Effect of Fairing on the Vortex Flows Around Airfoil/Flat-Plate Junctures," AIAA Paper 88-0615, Jan. 1988.

[12]Boermans, L. M. M. and Waibel, G., "Aerodynamic Design of the Standard Class Sailplane ASW-24," XX OSTIV Congress, Benalla, Australia, Jan. 1987.

[13]Ruszkowski, R. A., Jr., and Hallman, D., "The Study of the Effects of Wing-Body Integration on the Aerodynamic Interactions of a Sailplane Wing-Fuselage System," B. S. Thesis, The Pennsylvania State Univ., Dept. of Aerospace Engineering, March 1985.

[14]Chappel, G. G., Jr., and Waitz, I. A., "The Effects of Various Wing-Fuselage Integration Geometries on Total Sailplane Drag," B. S. Thesis, Pennsylvania State Univ., Dept. of Aerospace Engineering, May 1986.

[15]Kuchemann, D., *The Aerodynamic Design of Aircraft,* Pergamon, Oxford, 1978, pp. 266-289.

[16]Schlichting, H. and Truckenbrodt, E., *Aerodynamics of the Airplane,* McGraw-Hill, New York, 1979, Chap. 6.

[17]Stanbrook, A., "Experimental Observation of Vortices in Wing-Body Junctions," Aeronautical Research Council, R & M No. 3114, March 1959.

[18]Boermans, L. M. M. and Selen, H. J. W., "Design and Tests of Airfoils for Sailplanes with an Application to the ASW-19B," *Proceedings of the 13th Congress of the International Council of the Aeronautical Sciences,* Vol. 2, Aug. 1982, pp. 911-921.

[19]Rae, H. W. Jr. and Pope, A., *Low-Speed Wind Tunnel Testing,* 2nd ed., Wiley, New York, 1984, Chap. 6.

[20]Young, A. D., "Some Special Layer Problems," *Z. Flugwiss. Weltraumforsch,* Vol. 1, Nov.-Dec. 1977, pp. 401-414.